DELPHI 97-93 CONF 78
28 July, 1997

# A measurement of the cross section ratios and asymmetries for flavour tagged events at energies of 130 to 172 GeV and limits on new interactions

Preliminary

DELPHI Collaboration

**P.M. Kluit (NIKHEF, Amsterdam)**
CERN div. PPE, CH-1211 Geneva 23 Switzerland

**Abstract**

A measurement of the cross section ratios and forward-backward asymmetries for flavour tagged events in $e^+e^-$ annihilations at energies of 130 to 172 GeV has been performed with the DELPHI experiment at LEP. Hadronic events are selected and classified as bottom, charm and light quark events on the basis of the micro vertex detector information. The forward-backward asymmetry is measured using the jet charge. The cross sections ratios $R_q$, defined as the ratio of the cross section for one quark flavour to the total hadronic cross section, and the forward-backward asymmetries $A^q_{fb}$, measured for bottom, charm and light quark events are compared to the Standard Model expectations. No significant deviations from the Standard Model expectations are found. The data are interpreted in terms of possible new interactions that have been proposed to explain the events observed at HERA. Assuming a new contact interaction, limits on the coupling constant and mass scale $\Lambda$ of the interaction in the range from 1 to 4.4 TeV for the different quark species are derived.

Paper submitted to the LP'97 Conference
Hamburg, July 28 - August 1st

# 1 Introduction

Different models that assume the existence of new interactions and particles have been proposed to explain the events observed in the HERA experiments [1]. Some of these models have consequences for precision measurements that can be performed at the $e^+e^-$ collider LEP2 at energies of 130 GeV and higher [2, 3]. Generally, the existence of a new particle with a mass of around 200 GeV/c$^2$, will produce virtual effects at lower energies, and cross sections or forward-backward asymmetries might deviate from the Standard Model (SM) expectations. The measured cross sections and asymmetries for different quark flavours and lepton species at LEP2 might therefore - depending on the nature of the new interaction - be different from the Standard Model.

In this paper, the DELPHI measurements for the cross section ratios and forward-backward asymmetries for flavour tagged hadronic events at energies of 130 to 172 GeV will be presented. Hadronic events are selected and classified as bottom, charm, or light quark events on the basis on the micro vertex detector information. The forward-backward asymmetry is measured using the jet charge. The cross section ratio per quark flavour $R_q$ is defined, by analogy with $R_b$, as the ratio of the cross section for one quark flavour to the total hadronic cross section. The cross section ratios and asymmetries for bottom, charm and light quark events are compared to the Standard Model expectations.

Finally, the data are interpreted in terms of new interactions, and limits on coupling constants are derived. Firstly, supersymmetric models that have been proposed to explain the HERA data are discussed [4]. Secondly, in the hypothesis that new contact interactions exist, limits on the coupling constants and energy scales of the new interaction are obtained.

# 2 Event selection

The data taken by the DELPHI experiment at centre of mass energies of 130, 136, 161 and 172 GeV are analyzed, corresponding to an integrated luminosity of respectively 2.85, 2.98, 9.89 and 10.02 pb$^{-1}$. The 130-136 GeV data set was taken in 1995, the 161-172 GeV data set in 1996. The DELPHI detector and its performance are described in [5].

The selection of hadronic events follows closely the analysis described in [6]. First a selection for charged and neutral particles is applied. Tracks should have a momentum above 0.4 GeV/c, and a polar angle to the beam direction lying between 20 and 160 degrees. The relative error on the momentum should be less than 100%, and the track length at least 30 cm. The distance of closest approach to the beamspot should be less than 4 cm transverse to the beam line and 10 cm along it. For neutral particles, showers with an energy less than 1.5 GeV are rejected. Hadronic events are selected by requiring at least seven charged particles and that the charged particles carry at least 15% of the c.m.s. energy. To reject Bhabhas in the forward region, the energies in each endcap ($E_A$, $E_C$) of the forward calorimeter are calculated, and $ERAD = \sqrt{E_A^2 + E_C^2}$ is required to be less than 90% of the beam energy.

The thrust axis of the event is calculated including neutral particles, and its polar angle is required to be between 25 and 155 degrees. The charged and neutral particles are clustered into jets using the LUCLUS algorithm with an invariant mass cut of 5 GeV/$c^2$. To remove $W^+W^-$ events, only events with 3 jets or less are kept, with the additional requirement that all jets contain at least three particles. The effective c.m.s. energy $\sqrt{s'}$ is calculated using the SPRIME package [7]. To remove events that return radiatively to the Z, $\sqrt{s'}/\sqrt{s} > 0.85$ is required. A total sample of 360 hadronic events at a c.m.s. energy of 130 and 136 GeV, 299 events at 161 GeV and 263 events at 172 GeV was selected. The $W^+W^-$ background in the total sample amounts to 1.7% at 161 GeV and 6.2% at 172 GeV.

For the simulation, the DYMU3 and PYTHIA generator with DELPHI tuning are used to generate $q\overline{q}(\gamma)$ and $W^+W^-$ events [8, 9]. The simulated data set corresponds to more than 30 times the amount of real data.

# 3 Flavour tagging

The hadronic events are divided into three main classes on the basis of microvertex information. The first class is enriched in bottom quarks, the second in charm quarks and the third in light quarks. Tracks with microvertex detector hits are extrapolated to the primary vertex and the distance of closest approach to this vertex is determined with lifetime sign and its expected error. The probability ($P_E^+$) for the hypothesis that all the tracks in the event with a positive lifetime sign originate from the primary vertex is calculated [10]. If there are less than three tracks in the event with a positive lifetime sign, the event is not classified. Otherwise, the event is classified as bottom if $P_E^+$ is less than 0.002, as charm if $P_E^+$ is between 0.002 and 0.1, and as light quark if $P_E^+$ is larger than 0.1. These cuts were chosen to optimize the efficiency and purity for the different categories. The efficiencies and purities after this classification for the energies of 161-172 GeV with $\sqrt{s'}/\sqrt{s} > 0.85$ obtained by simulation are shown in Table 1.

| tag | efficiency | b content | c content | uds content |
|---|---|---|---|---|
| bottom | 0.67 (b) | 0.77 | 0.18 | 0.05 |
| charm | 0.33 (c) | 0.17 | 0.40 | 0.43 |
| light quark | 0.76 (uds) | 0.03 | 0.23 | 0.74 |

Table 1: Efficiencies and purities for the different tags at energies of 161-172 GeV.

In order to reduce the systematic errors, the hadronic Z data are used to check the three tags. For the 1995 data 41k selected events were used, for the 1996 data 21k. The fractions of tagged events in data and simulation were compared and their ratios were found to be $0.942 \pm 0.010$ ($1.008 \pm 0.017$) for the b tag, $1.046 \pm 0.010$ ($1.076 \pm 0.017$) for the c tag, and $1.006 \pm 0.005$ ($0.977 \pm 0.010$) for the light quark tag. The numbers in brackets correspond to the Z data taken in 1996, the errors are statistical only. The tagging rates agree within better than 10% with the values from the simulation. To obtain precise predictions for the tagging rates above 130 GeV, the observed rates were corrected using these fraction. It is assumed that the fractions of bottom, charm and light quark events at the Z are the same as predicted in the Standard Model. This procedure reduces substantially the systematic errors affecting the quark cross section ratios at energies above 130 GeV.

# 4 Measurement of cross section ratios and asymmetries

The cross section ratios $R^{obs}$ for the different tags are obtained by dividing the number of tagged events by the total number of bottom, charm and light quark tagged events. The same procedure is applied for real and simulated data. The results for the observed cross section ratio $R^{obs}$ minus the expected ratio for the Standard Model, i.e. the value obtained for the simulated data, divided by the expected ratio are shown in Table 2 for the different tags together with the total error and the systematic contribution.

| tag (energy) | events | $(R^{obs} - R^{SM})/R^{SM}$ | total error | syst. error |
|---|---|---|---|---|
| bottom (130-136 GeV) | 58 | -0.132 | 0.132 | 0.012 |
| charm (130-136 GeV) | 58 | -0.102 | 0.132 | 0.014 |
| light quark (130-136 GeV) | 212 | 0.078 | 0.072 | 0.02 |
| bottom (161-172 GeV) | 78 | -0.105 | 0.11 | 0.018 |
| charm (161-172 GeV) | 108 | -0.019 | 0.098 | 0.020 |
| light quark (161-172 GeV) | 322 | 0.036 | 0.059 | 0.022 |

Table 2: Deviation of the observed rates w.r.t. the Standard Model for the different tags at energies of 130-136 and 161-172 GeV with $\sqrt{s'}/\sqrt{s} > 0.85$.

The systematic error listed in the last column of Table 2 has two components. The first is due to the statistical uncertainty coming from the normalization to the hadronic Z data. The second is due to the discrepancies between data and simulation at the Z. To propagate these uncertainties, it is assumed that the bottom, charm and light quark efficiencies in the simulation have an uncertainty of at most 10%. The error on the expected tagging rate was then evaluated by taking the worst case scenarios, e.g. where discrepancies for the light quark tag were fully attributed to presence of charm background. The quadratic sum of these two components is quoted as the total systematic error.

The results for the observed rates are compatible within approximately one standard deviation with the rates expected in the Standard Model.

At the Z pole the forward-backward asymmetries for quarks are at most 0.10. At centre of mass energies of 161-172 GeV, one expects much larger forward-backward asymmetries of typically 0.66 and 0.54 for up and down type quarks respectively. To measure the forward-backward asymmetries for different quark flavours, the jet charge is used. The jet charge is sensitive to the initial quark charge and is defined in the following way [11]:

$$Q_{jet} = \sum_i q_i p_{i//}^{\kappa} / \sum_i p_{i//}^{\kappa} \tag{1}$$

with $\kappa = 0.6$, $p_{i//}$ the momentum component along the thrust axis, and $i$ runs over the tracks in one hemisphere, defined by the thrust axis. The forward-backward jet charge $Q_{fb}$ is defined as the difference of the forward minus the backward jet charge. Events with a $Q_{fb}$ larger than 0.2 or less than -0.2 are selected, and the direction of the thrust axis is signed accordingly. The angular distribution can be described by:

$$\frac{d\sigma}{d\cos\theta_t} = 1 + A\cos^2\theta_t + (6+2A)/3\; A_{fb}\cos\theta_t, \tag{2}$$

where $\theta_t$ is the signed polar angle of the thrust axis and $A_{fb}$ the forward-backward charge asymmetry. For $A$ a value of 1 is chosen. The angular distribution will be fitted in the range $|\cos\theta_t| < 0.8$. The charge asymmetry is positive for charm and up quarks, and negative for bottom, strange and down quarks.

The observed asymmetry $A_{fb}^{obs}$ will be reduced because the jet charge sometimes gives the wrong sign. This can be expressed by a charge confusion factor $C$, according to the following equation:

$$A_{fb}^{obs} = C A_{fb}. \tag{3}$$

Using the simulation, the constant $C$ is determined to be 0.54 for bottom, 0.37 for charm, 0.55 for strange, 0.62 for up, and 0.52 for down quarks at energies of 161-172 GeV. The angular distributions at energies of 161-172 GeV for all events and for bottom, charm and light quark tagged events are shown together with the fitted curves in Figure 1. The grey areas give the Standard Model predictions from the simulation.

The results for the different tags at energies of 130-136 and 161-172 GeV for the observed asymmetry minus the asymmetry expected in the Standard Model are shown in Table 3.

| tag (energy) | $A_{fb}^{obs} - A_{fb}^{SM}$ | total error | syst. error |
|---|---|---|---|
| all (130-136 GeV) | -0.115 | 0.074 | 0.002 |
| bottom (130-136 GeV) | -0.068 | 0.171 | 0.020 |
| charm (130-136 GeV) | -0.108 | 0.178 | 0.010 |
| light quark (130-136 GeV) | -0.144 | 0.099 | 0.015 |
| all (161-172 GeV) | 0.029 | 0.057 | 0.002 |
| bottom (161-172 GeV) | -0.009 | 0.174 | 0.020 |
| charm (161-172 GeV) | -0.283 | 0.115 | 0.010 |
| light quark (161-172 GeV) | 0.142 | 0.074 | 0.010 |

Table 3: The observed forward-backward charge asymmetry minus the Standard Model expectations for the different tags at energies of 130-136 and 161-172 GeV with $\sqrt{s'}/\sqrt{s} > 0.85$.

The systematic error listed in the last column comes from two sources. Firstly, from a 15% uncertainty on the charge confusion factors $C$. Secondly, the discrepancies between data and simulation observed in the tagging rates at the Z are propagated according to the method described above.

The results for the forward-backward asymmetries are in agreement with the Standard Model expectation, except for the rather low value of the asymmetry for charm tagged events in the 161-172 GeV data. To compute the charm asymmetry, the charm purity was used. It can be argued that if the bottom, charm or light quark rates differ from the Standard Model predictions, the purities - and thus the asymmetries - would be wrong. But from Table 2 it can be concluded that the tagging fractions agree very well with the Standard Model predictions. Thus the low charm asymmetry cannot be explained in this way.

Possible detector effects were carefully studied. Several distributions were checked using the higher statistics Z data, e.g. by comparing the jet charge in the forward region and the $s'$ distributions with the simulation. The distributions were consistent with the expectations from the simulation. Further, the observed forward-backward charge asymmetries at the Z were compared to the Standard Model expectations for flavour tagged events and found to be $A_{fb}^{obs} - A_{fb}^{SM}$ = -0.023 ± 0.012 (all), -0.019 ± 0.038 (bottom), -0.008 ± 0.033 (charm) and -0.039 ± 0.022 (light quarks), consistent with expectations.

As a further cross check, the value of $\kappa$ was changed to 1 for the 161-172 GeV data, and the cut on the jet charge difference $Q_{fb}$ was adjusted to 0.3 to accept the same amount of events. The result for the asymmetry difference $A_{fb}^{obs} - A_{fb}^{SM}$ was 0.062 ± 0.057 (all), -0.137 ± 0.17 (bottom), -0.213 ± 0.12 (charm), and 0.175 ± 0.074 (light quarks), consistent with the results listed in Table 3. No anomaly was found and it was concluded that the low asymmetry for charm tagged events is not due to a detector effect.

From the measured cross section ratios and asymmetries it is possible to extract cross section ratios and asymmetries for bottom, charm, strange, up and down quarks. To extract the cross section for one quark flavour, the cross sections for the other flavours are taken from the Standard Model. To extract the forward-backward asymmetry for one quark flavour, the cross sections and asymmetries for the other flavours are taken from the Standard Model. The result of this procedure is given in Table 4.

| quark flavour (energy) | $(R_q - R^{SM})/R^{SM}$ | total error | $A_{fb}^{q} - A_{fb}^{SM}$ | total error |
|---|---|---|---|---|
| bottom (130-136 GeV) | -0.17 | 0.17 | 0.21 | 0.52 |
| charm (130-136 GeV) | -0.26 | 0.33 | -0.75 | 1.2 |
| light (130-136 GeV) | 0.11 | 0.10 | | |
| down (130-136 GeV) | 0.34 | 0.31 | 0.95 | 0.65 |
| up (130-136 GeV) | 0.26 | 0.24 | -0.75 | 0.52 |
| strange (130-136 GeV) | 0.38 | 0.35 | 0.78 | 0.54 |
| bottom (161-172 GeV) | -0.13 | 0.15 | 0.02 | 0.41 |
| charm (161-172 GeV) | -0.05 | 0.25 | -1.91 | 0.78 |
| light (161-172 GeV) | 0.05 | 0.08 | | |
| down (161-172 GeV) | 0.16 | 0.26 | -1.19 | 0.62 |
| up (161-172 GeV) | 0.12 | 0.20 | 0.75 | 0.39 |
| strange (161-172 GeV) | 0.18 | 0.29 | -1.25 | 0.64 |

Table 4: The derived quark cross section ratio and forward-backward quark asymmetry difference w.r.t the Standard Model for different flavours at energies of 130-136 and 161-172 GeV with $\sqrt{s'}/\sqrt{s} > 0.85$.

Note that a minus sign is used to convert the observed charge asymmetry into the forward-backward quark asymmetry for bottom, strange and down quarks. The value for the charm asymmetry difference at 161-172 GeV is slightly lower than the physically allowed minimum of $-1.66$ (this minimum arises because the measured charm asymmetry cannot be lower than $-1$ while the Standard Model expectation is 0.66).

The forward-backward asymmetry for bottom quarks $A_{fb}^{b}$ is $0.69 \pm 0.52$ at 130-136 GeV and $0.57 \pm 0.41$ at 162-172 GeV. This may be compared with 0.10 at the Z. Thus the DELPHI data confirm the expected rise of the forward-backward asymmetry for bottom quarks as a function of the centre of mass energy. More data is needed to check the

Standard Model predictions more precisely. From the results listed in Table 4, it is possible to extract the cross section ratios for bottom, charm and light quark events, as shown in Table 5. The ratios do not add up exactly to unity, because the purities are taken from the simulation. In Figure 2, the cross section ratios for bottom, charm and light quarks are shown as a function of the centre of mass energy, together with the predictions from ZFITTER [12].

| quark flavour (energy) | $R_q$ | total error |
|---|---|---|
| bottom (130-136 GeV) | 0.151 | 0.031 |
| charm (130-136 GeV) | 0.167 | 0.074 |
| light (130-136 GeV) | 0.656 | 0.059 |
| bottom (161-172 GeV) | 0.143 | 0.024 |
| charm (161-172 GeV) | 0.237 | 0.061 |
| light (161-172 GeV) | 0.614 | 0.047 |

Table 5: The derived quark cross section ratios for different flavours at energies of 130-136 and 161-172 GeV with $\sqrt{s'}/\sqrt{s} > 0.85$.

The measurements are in agreement with the Standard Model, except for the charm asymmetry at 161-172 GeV, which is rather low. A comparison with the results of the other LEP experiments or the inclusion of the data that will be taken in 1997, will make it clear whether this deviation is significant or just a statistical fluctuation.

# 5 Interpretations

From the hadronic cross sections at 130 to 172 GeV measured by DELPHI [6] and the results for the flavour tagged cross section ratios and asymmetries given above, limits on new interactions can be derived. Firstly, the interpretation of the HERA data in terms of the following three possible processes [4] is considered : (i) $e^+d \rightarrow \tilde{u}_L$, (ii) $e^+s \rightarrow \tilde{u}_L$ or (iii) $e^+\bar{u} \rightarrow \tilde{d}_R$, where a valence down quark, a strange sea quark or anti-up sea quark is interacting, respectively, and producing a left-handed up-type or right-handed down-type squark. Secondly, more general limits on contact interactions will be obtained.

In $e^+e^-$ interactions, a quark-antiquark pair is produced through the exchange of a photon or $Z^0$. If a new interaction exists, $e^+e^-$ pairs can annihilate through the exchange of a leptoquark or squark of mass $m$ and coupling constant $\lambda$ in the t-channel, and produce a quark-antiquark pair. The production cross sections and asymmetries for quarks are then affected, mainly due to the interference of this new process with SM processes.

The results given below are based on the formalism of [2], for two solutions [1] that fit in the framework of supersymmetry, assuming that R parity is not conserved. Other forms of the interaction that involve a leptoquark are discussed below. In the calculations, the effects of initial and final state radiation and higher order contributions are neglected. Assuming a squark mass of 200 GeV/c$^2$, the cross sections and asymmetries for different

[1] An $LR$, $\alpha = -1/2$ interaction for up type quarks and an $LL$, $\alpha = +1/2$ for down type quarks, see Eq.(4), and [2].

values of $\lambda$ for down (up) type quarks in the final state are given in Figure 3 for a centre of mass energy of 166 GeV. For final states with down type quarks, the cross section increases as a function of $\lambda$; for up type quarks, the cross section first decreases and then increases due to the interference.

The 95 % upper limits on the cross section ratios $\sigma - \sigma^{SM}/\sigma^{SM}$ are calculated from the different cross section ratios given in Table 2, the efficiencies and purities given in Table 1, the ratios of u:d:s quarks expected in the light quark sample, and the mean value of the ratio of the measured hadronic cross section $\sigma^h$ w.r.t. the Standard Model for $\sqrt{s'}/\sqrt{s} > 0.85$ at centre of mass energies of 130-136 GeV and 161-172 GeV [6]. The results are compared with the model predictions in Fig. 3.

It can be seen that a coupling constant $\lambda$ larger than 0.87 for strange, 0.81 for down, and 0.62 for bottom quarks can be excluded at 95 % CL. On the basis of the forward-backward asymmetry, $\lambda$ values larger than 0.87 can be excluded for bottom quarks. For up (charm) quarks a coupling constant larger than 1.24 is excluded at 95 % CL, and coupling constants between 0.43(0.47) and 1.02(1.00). For up quarks, the region between 1.02 and 1.24 is excluded by the 130-136 GeV data, and thus $\lambda$ values above 0.43 are excluded. For processes (i) and (ii) one would expect a $\lambda$ value of 0.1 $\pm$ 0.05 for down quarks and 0.5 $\pm$ 0.25 for strange quarks respectively [4]. For process (iii) one expects $\lambda$ to be 0.4 $\pm$ 0.2 for anti-up quarks. Only the third process is constrained by DELPHI data.

| interaction | d or s $\lambda$ | b $\lambda$ | u or c $\lambda$ | d or s $\Lambda$ (TeV) | b $\Lambda$ (TeV) | u or c $\Lambda$ (TeV) |
|---|---|---|---|---|---|---|
| $LL+$ | 0.33 | 0.16 | 0.72 | 2.2 | 4.4 | 1.0 |
| $LL-$ | 0.25 | 0.18 | 0.32 | 2.8 | 3.9 | 2.2 |
| $LR+$ | 0.46 | 0.29 | 0.53 | 1.5 | 2.4 | 1.3 |
| $LR-$ | 0.50 | 0.36 | 0.43 | 1.4 | 2.0 | 1.7 |
| $RR+$ | 0.41 | 0.23 | 0.63 | 1.7 | 3.1 | 1.1 |
| $RR-$ | 0.55 | 0.43 | 0.37 | 1.3 | 1.7 | 1.9 |
| $RL+$ | 0.55 | 0.43 | 0.48 | 1.3 | 1.7 | 1.5 |
| $RL-$ | 0.42 | 0.24 | 0.48 | 1.7 | 3.0 | 1.5 |

Table 6: Upper limits at 95% CL on the coupling constant $\lambda$ and energy scale $\Lambda$ for different forms of the interaction for down or strange quarks, bottom quarks, and up or charm quarks.

It is possible to obtain more general limits on contact interactions. These scenarios cover also the exchange of a leptoquark or squark. For this purpose the effective Lagrangian is used [2]:

$$L_{eff} = \sum_{i,k=L,R} \lambda_{ik}^2/m^2 \alpha^{ik} (\bar{e}_i \gamma^\mu e_i)(\bar{q}_k \gamma^\mu q_k) \quad (4)$$

with $\alpha^{ik}$ equal to $\pm 1$, and $e_i$, $q_k$ denoting the right-handed (R) and left-handed (L) electron and quark fields. The cross sections and asymmetries were evaluated for final states with up and down type quarks assuming a mass $m$ of 200 GeV/c$^2$. The coupling constant

$\lambda$ was varied for the $LL$, $LR$, $RR$ and $RL$ final states and for the two $\alpha$ values, giving eight curves for the cross sections and asymmetries. The new interaction was assumed to couple to only one quark and with only one form of the coupling, i.e. either $LL+$ or $LL-$, etc. The result is shown in Figure 4. The dashed curves give asymptotically a negative forward-backward asymmetry. For some of the curves, the helicity states and $\alpha$ values are indicated. The limits at 95% CL on the coupling constant $\lambda$ for strange and down quarks and for up and charm quarks are listed in Table 6 for the different forms of the interaction.

The limits for bottom quarks are better than the limits for the down or strange quarks. The limits on the coupling constant scale approximately linearly with the mass $m$.

The effective Lagrangian can also be expressed in terms of the energy scale $\Lambda$ of the interaction, where $\Lambda^2 = \frac{4\pi m^2}{\lambda^2}$ [2]. The corresponding limits at 95% CL are also given in Table 6. The limits on $\Lambda$ are in the range from 1 to 4.4 TeV.

# 6 Conclusions

The cross sections ratios and asymmetries for different quark flavours have been measured for the data taken at the energies of 130 to 172 GeV. The results are in agreement with the expectations from the Standard Model, except for the charm asymmetry at energies of 161-172 GeV which is rather low. This result should be confirmed by the data that will be taken in 1997. The data were interpreted in terms of possible new interactions. First, interactions were considered that could offer an explanation for the events observed at HERA and exclusion limits were derived. Secondly, more general contact interactions were considered and limits on the coupling constants and mass scales in the range from 1 to 4.4 TeV were obtained for different quarks.

# Acknowledgement

The author would like to thank Francois Richard for stimulating discussions.

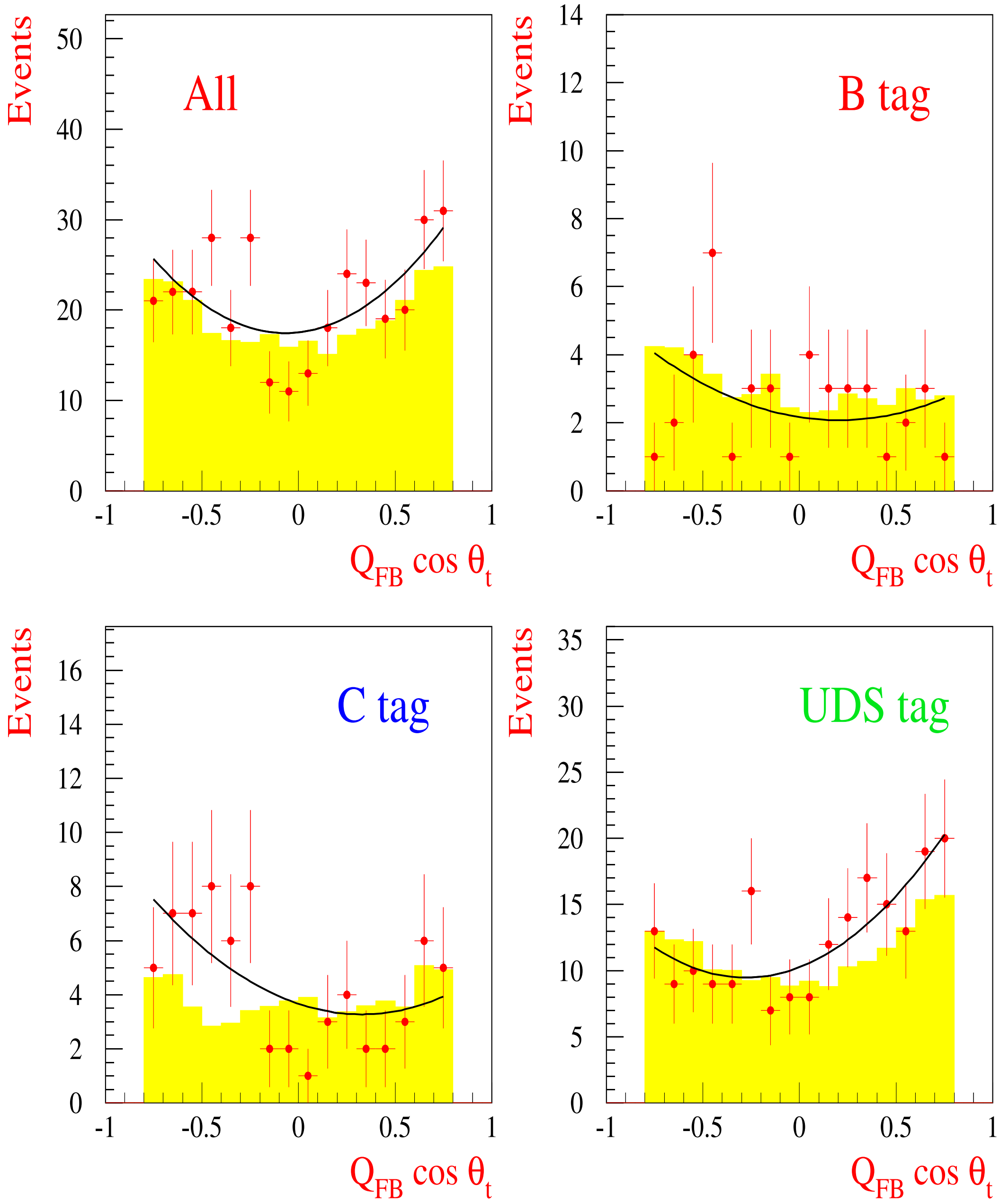


Figure 1: The charge-signed polar angle distributions for all events, bottom, charm and light quark tagged events at energies of 161-172 GeV. The grey area gives the Standard Model prediction, the dots with error bars represent the data, the solid line the fitted curve to the data of Eq.(2).

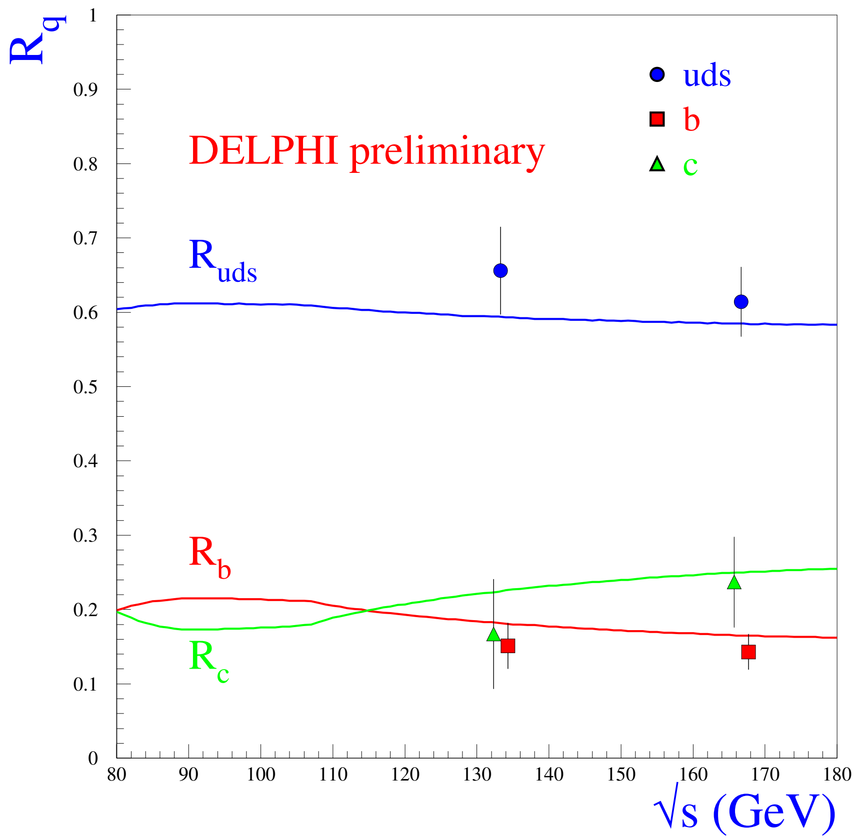


Figure 2: The measured cross section ratios for bottom, charm and light quarks as a function of the centre of mass energy, together with the predictions from ZFITTER.

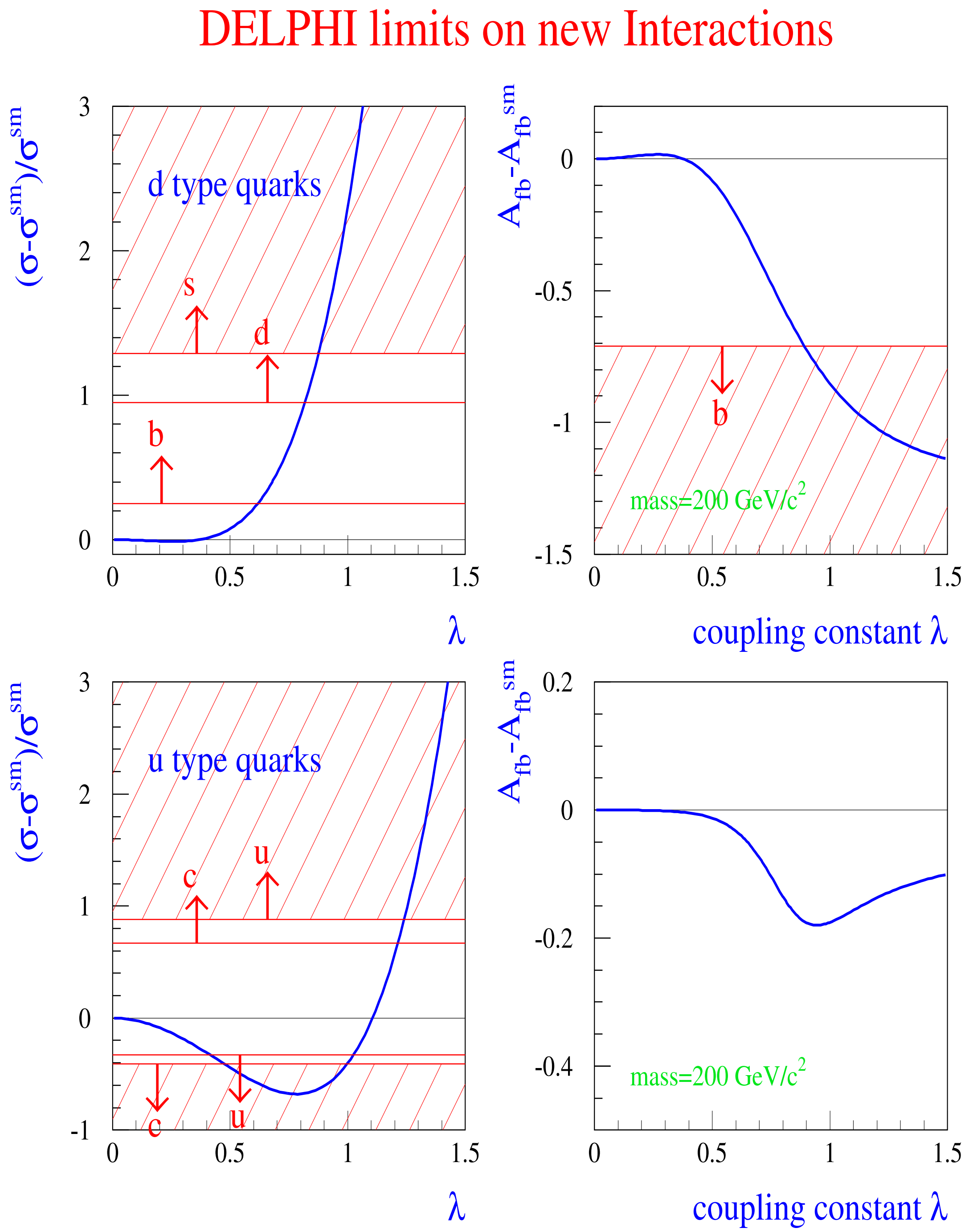


Figure 3: The expected cross section ratio and asymmetry difference as a function of the coupling constant $\lambda$ for down (upper plot) and up (lower) type quarks, assuming a squark with a mass of 200 GeV/c$^2$ for processes (i) to (iii). The horizontal lines and the hatched area correspond to the different exclusion limits at 95 % CL. The arrow points to the excluded zone.

# DELPHI limits on new Interactions

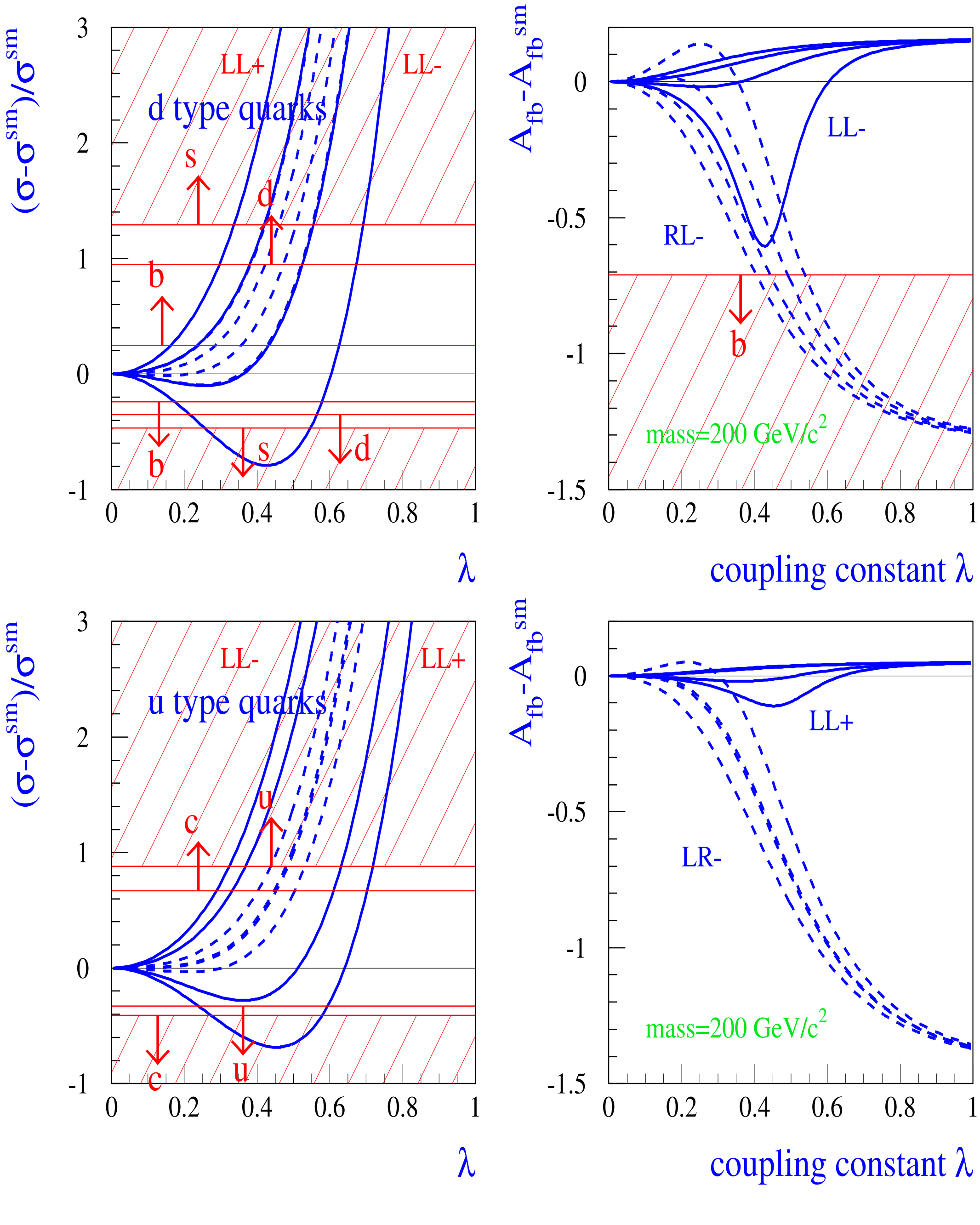


Figure 4: The expected cross section ratio and asymmetry difference as a function of the coupling constant $\lambda$ for down (upper plot) and up (lower) type quarks, assuming a new interaction of the form Eq.(4) with a mass of 200 GeV/c$^2$. The dashed curves, give asymptotically a negative forward-backward asymmetry. The eight curves correspond to the different helicity states. The horizontal lines and the hatched area correspond to the different exclusion limits at 95 % CL. The arrow points to the excluded zone.

# References


[1] C. Adloff et al. (H1 Collaboration), *Observation of events at very high $Q^2$ in ep collisions at HERA*, DESY 97-024, submitted to Z. Phys. C;
J. Breitweg et al. (Zeus Collaboration), *Comparison of ZEUS data with Standard Model predictions for $e^+p^- \to e^+X$ scattering at high $x$ and $Q^2$*, DESY 97-025, submitted to Z. Phys. C.

[2] J. Kalinowski et al., *Leptoquark/Squark interpretation of HERA events; virtual effects in $e^+e^-$ annihilation to hadrons*, DESY 97-038.

[3] G. Altarelli, *Pursuing interpretations of the HERA large-$Q^2$ data*, CERN-TH/97-040;
D. Choudhury, Phys Lett. **B376** (1996) 201.

[4] F. Richard, *Possible implications at LEP2 of the effect seen at HERA*, DELPHI 97-46 PHYS 698.

[5] P. Aarnio et al. (DELPHI Collaboration), Nucl. Instr. Meth. **A 303** (1991) 233;
P. Abreu et al., Nucl. Instr. Meth. **A 378** (1996) 57.

[6] A. Behrmann et al. (DELPHI Collaboration), *DELPHI results on the measurement of fermion-pair production for $Z^0$ peak and higher energies at LEP for the Winter Conferences*, DELPHI note 97-31 PHYS 684.

[7] P. Abreu et al., *SPRIME a package for estimating the effective $\sqrt{s'}$ centre of mass energy in $q\bar{q}\gamma$ events*, DELPHI 96-124 PHYS 632.

[8] J.E. Campagne and R.Zitoun, Z. Phys. **C43** (1989) 469.

[9] T. Sjöstrand, Comp. Phys. Comm. **39** (1986) 347; T. Sjöstrand, *PYTHIA 5.7 and JETSET 7.4*, CERN-TH 7112/93.

[10] P. Abreu et al. (DELPHI Collaboration), Zeit. Phys. **C70** (1996) 531;
G. Borisov and C. Mariotti, *Performance of b-tagging at LEP2*, DELPHI 97-16 PHYS 672.

[11] P. Abreu et al. (DELPHI Collaboration), Phys. Lett. **B322** (1994) 459.

[12] D. Bardin et al., CERN-TH 6443 (1992) and references therein.